Study of Fuel-Pusher Mixing in Laser-Driven Implosions, Using Secondary Nuclear Fusion Reactions

H. Azechi, R. O. Stapf, N. Miyanaga, R. Tsuji, M. Yamanaka, S. Ido, K. Nishihara, T. Yabe, and C. Yamanaka

Institute of Laser Engineering, Osaka University, Suita, Osaka 565, Japan

(Received 27 July 1987)

Ablative implosions of glass microballoon targets driven by twelve 0.53-μm laser beams have been studied by use of secondary DT and D ^{3}He fusion reactions in an initially pure deuterium fuel. The tritons and ^{3}He nuclei are products of primary DD fusion reactions. Comparisons with results of a hydrodynamic simulation indicate that collisional energy loss for these primary fusion products is strongly enhanced by fuel-pusher mixing taking place during the implosion.

PACS numbers: 52.50.Jm, 25.55.−e, 52.70.Nc

A current topic of interest in studies of high-density compression for inertial-confinement fusion is the stability of shell targets during implosions. Nonuniformity of laser irradiation and/or hydrodynamic instabilities may seriously limit the compressed fuel density by fuel-pusher mixing or, in a moderate case, nonuniform compression. Some direct evidence of fuel shape deformation has been observed by α-particle imaging.[1] However, to date no experimental study of fuel-pusher mixing has been carried out. In this Letter we present results of charged-particle energy-loss measurements in the compressed fuel by use of secondary nuclear fusion reactions.[2–8] This method permits a study of fuel-pusher mixing in dense, compressed fuel.[7]

Simultaneous yield measurements were carried out for primary DD neutrons, secondary DT neutrons, and secondary D ^{3}He protons generated in an initially pure deuterium fuel. The tritons and ^{3}He nuclei are first generated by primary DD reactions. Throughout this work, it is assumed that the yields of DD neutrons and DD protons are the same. After the tritons and ^{3}He nuclei suffer significant energy loss in the fuel, the DT cross section increases from the value at the triton birth energy (1.01 MeV) to a peak value at 0.17 MeV. In contrast, the D ^{3}He cross section decreases (except for a small initial increase) with decreasing ^{3}He energy from the value at the ^{3}He birth energy (0.82 MeV). Therefore, the yield ratio of the secondary D ^{3}He protons to the secondary DT neutrons Y_{2p}/Y_{2n} becomes a direct function of the energies of tritons and ^{3}He nuclei after their escape from the fuel. This ratio is only weakly dependent on fuel temperature and density. The calculated behavior of Y_{2p}/Y_{2n} as a function of the escaping triton energy[8] E_T is shown in Fig. 1. For this calculation it was assumed that primary fusion products are uniformly produced in the spherical fuel with uniform temperature and density profiles. Since the escaping tritons have a broad energy distribution in this model, a characteristic triton energy is calculated for tritons traversing one fuel radius. For the energy-loss calculation, we used a standard expression for the charged-particle stopping power in a fully ionized plasma.[9]

With the triton energy known from this ratio, the fuel areal density and the electron temperature can be determined from the yield ratio of the secondary DT neutrons to the primary DD neutrons Y_{2n}/Y_{1n}. This is shown in Fig. 2. For a given escaping triton energy, the yield ratio Y_{2n}/Y_{1n} can be shown as a function of the fuel areal density [Fig. 2(a)] and of the electron temperature [Fig. 2(b)]. [In this calculation, the electron temperature range was limited between 0.1 and 10 keV, resulting in the termination of the curves in the middle of the graph of Fig. 2(a).]

If fuel-pusher mixing takes place, the energy loss is enhanced by enrichment of the charged-particle density in the fuel. Since the fuel areal density $\rho_D R$ can be

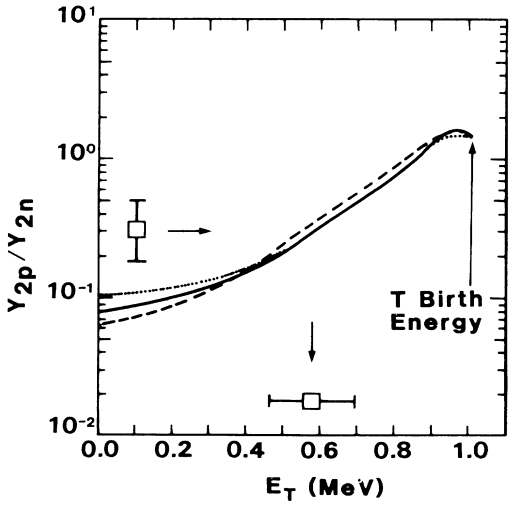

FIG. 1. Yield ratios of secondary D ^{3}He protons to secondary DT neutrons as a function of the triton energy after traversal of one fuel radius for $T_{\text{eff}}=0.1$ keV (dashed line), $T_{\text{eff}}=1$ keV (solid line), and $T_{\text{eff}}=10$ keV (dotted line). Density dependence is negligibly small for $\rho_D=0.1-10$ g/cm^3.

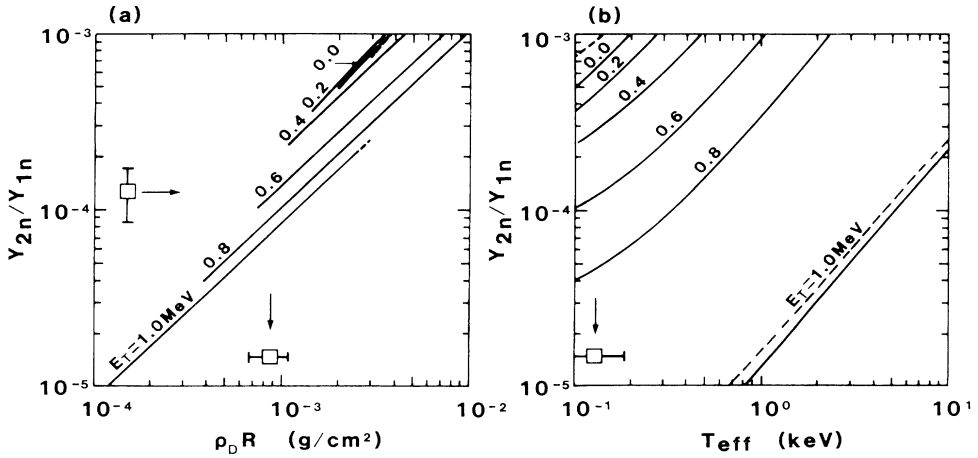

FIG. 2. Yield ratio of secondary DT neutrons to primary DD neutrons as a function of (a) fuel areal density and (b) effective electron temperature for $\rho_D = 0.1$ g/cm^3 (solid line) and $\rho_D = 1.0$ g/cm^3 (dashed line). The parameter is the escaping triton energy.

determined even with mixing taking place, the electron temperature determined above may be regarded as an "effective" temperature, T_{eff}. This temperature together with the $\rho_D R$ value characterizes the energy loss. In the following, we show that the observed effective temperature is much lower than results of hydrodynamic simulation, thereby indicating that fuel-pusher mixing takes place.

Experiments were performed at the twelve-beam Nd-doped glass laser facility, Gekko XII, at Osaka University. Experimental conditions are summarized in Table I. Targets were glass microballoons filled with pure deuterium gas plus ~0.1 atm residual gas (mainly nitrogen). Surface roughness of the targets was nearly 0.02 μm for wavelengths of the order of the shell thickness. The targets were irradiated by 0.53-μm laser radiation having a Gaussian pulse shape of 0.8 ns duration (full width at half maximum) focused through $f/3$ lenses. The laser foci were positioned beyond the target center by 5 times the target radius in order to reduce the irradiation nonuniformity. The standard deviation of the laser intensity distribution on the target was approximately 25% of the average intensity.

To measure the yield of the secondary DT neutrons, we used a time-of-flight (TOF) detector[3,4] located 1.1 or 1.5 m from the target. In addition, a Na activation counter[3,4] was used. (The Cu activation counter used in Refs. 3 and 4 was not used in this study because of uncertain background measurements.) For D ^{3}He proton detection, CR-39 nuclear track detectors[5] were used. The lowering of the observed D ^{3}He proton yield because of collisional energy loss in the target is negligible for a fuel areal density of $\simeq 1$ mg/cm^2 (see Table II) and a pusher areal density of $\simeq 9$ mg/cm^2 (observed by pusher-activation method for the same experimental conditions as those in this study but with use of DT fuel[4]). These detectors were absolutely calibrated to $\pm 14\%$ (CR-39), $\pm 15\%$ (TOF), and $\pm 3\%$ (Na activation) accuracy. The uncertainty due to the angular distribution of the secondary reaction products was estimated[4,5] to be roughly $\pm 30\%$ by the use of two CR-39 detectors and two neutron detectors positioned at different viewing directions. Uncertainties including statistical errors, etc., were calculated for each result. The primary DD neutron yield was measured with an absolutely calibrated Ag-activation counter[10] (uncertainty is $+6\%, -9\%$). Fuel ion temperatures were also measured with a neutron TOF spectrometer located 16 m from the target. Time-integrated x-ray images of the target were monitored by x-ray pinhole cameras having response to 2–3-keV x rays. Strong x-ray emission from the fuel region, as well as from the stagnated pusher region, was observed (not shown here).

TABLE I. Experimental conditions.

Target name	Outer diameter (μm)	Wall thickness (μm)	Deuterium pressure (atm)	Laser energy (kJ)	Pulse width (ns)
A	752	2.03	13	5.9	0.8
B	715	2.05	13	6.7	0.8

A benchmark test[5] had been carried out to confirm that the experimental apparatus was working properly. There, the secondary yield ratio of $Y_{2p}/Y_{2n} \simeq 2$ had been observed for a thinner target (1.3-μm thickness). This Y_{2p}/Y_{2n} value is consistent with the theoretical prediction of $Y_{2p}/Y_{2n} \simeq 1.6$ for a small energy loss of the tritons (see Fig. 1). (The small energy loss in the benchmark test is probably due to a higher temperature, lower areal density, and/or less violent mixing, which may be explained by a decreased in-flight-aspect ratio due to shell preheating.)

Experimental and calculated results are summarized

TABLE II. Experimental and simulation results. The latter are in the square brackets. Y_{1n}, primary DD neutron yield; Y_{2n}, secondary DT neutron yield; Y_{2p}, secondary D ^{3}He proton yield; E_T, escaping triton energy; $\rho_D R$, fuel areal density; T_{eff}, effective electron temperature (see text); T_{calc}, calculated electron temperature by simulation; T_i, ion temperature.

Target name	Y_{1n}	Y_{2n}	Y_{2p}	E_T (MeV)	$\rho_D R$ (mg/cm^2)	T_{eff} [T_{calc}] (keV)	T_i (keV)
A	1.1×10^{10}	$(1.4\pm0.5)\times10^6$	$(4.4\pm1.5)\times10^5$	0.58 ± 0.11	0.87 ± 0.20	$0.13^{+0.05}_{-0.06}$	4.7 ± 0.9
	[1.9×10^{10}]				[5.1]	[1.7]	[3.2]
B	6.4×10^9	$(7.3\pm2.6)\times10^5$	$(5.2\pm1.8)\times10^5$	$0.76^{+0.11}_{-0.12}$	$1.1^{+0.23}_{-0.35}$	$0.30^{+0.16}_{-0.11}$	5.1 ± 1.0
	[2.6×10^{10}]				[5.6]	[1.9]	[3.5]

in Table II. In contrast to the benchmark result, the yield ratios Y_{2p}/Y_{2n} are lower than unity. For target A, values for E_T as well as $\rho_D R$ and T_{eff} are also shown in Figs. 1 and 2 by data points. Uncertainties for these values were calculated by the variation of values for Y_{2n} and Y_{2p} within an ellipse on a Y_{2p}-Y_{2n} plane with radii equal to their uncertainties. The uncertainty of Y_{1n} was insignificant. For target B, a higher T_{eff} value arises partly as a result of the larger laser energy and the smaller target mass.

Observed effective temperatures were compared with results of our one-dimensional Lagrangean hydrodynamic code HIMICO[11] with use of a flux-limit factor of $f=0.05$. The simulation results of fuel areal density and electron and ion temperatures which are listed in Table II were calculated at the peak thermonuclear burn. Measured ion temperatures are only slightly higher than the calculated results (averaged by weighting of neutron yield from each Lagrangean mesh). But the effective temperatures are much lower than the calculated electron temperature (averaged over total electron number in the fuel) by factors of 13 and 6.3 for targets A and B, respectively. This discrepancy indicates an enhanced energy loss of the tritons.

We considered several possibilities for the electron-temperature discrepancy. Contribution of the originally mixed residual gas to the energy loss was calculated to be only $\simeq5\%$ of the deuteron contribution. An amount of deuterium remaining within the glass material was negligibly small to affect the secondary-reaction yields.

It is unlikely that the calculated electron temperature is seriously overestimated. For example, in target A the calculated electron temperature for underestimated flux limitation of $f=0.02$ was still 7.3 times higher than the observed effective temperature.

It is possible that the electron temperature was overestimated by incorrect prediction of the peak burn time. A lower electron temperature is expected if peak burning occurs near the time when the shock wave in the fuel first collapses at the target center. However, when we calculated the electron temperature at the shock collapse time, the value was still 6.5 times higher than the effective temperature.

It is also unlikely that the observed effective temperature is too low because of uncertainties in the model assumptions. We considered the central spark model, where the primary fusion products are generated at the center of the fuel. This model yields a lower experimental value for T_{eff}, making the discrepancy even larger. Furthermore, addition of a nonuniform temperature profile having a peak at the target center also yields a lower T_{eff} value.

The electron temperature discrepancy could arise from the theoretical uncertainty of electron-ion Coulomb logarithm $\ln\Lambda$ in the energy-loss calculation. However, this uncertainty is estimated to be only of the order of $1/\ln\Lambda\simeq\frac{1}{4}$ even for the largest uncertainty case (target A) and is too small to explain the discrepancy.

The enhancement of the energy loss due to fuel shape deformation is possible only if most of the primary products are generated in convex regions of the fuel, and then pass through the pusher to react with deuterons in other convex regions. This situation is unlikely to occur, because from a geometrical consideration only a small amount of the primary products can doubly pass the fuel.

Therefore, the reduced effective temperature is most likely due to fuel-pusher mixing. This mixing also explains the lower areal density and DD neutron yields compared to the simulation results (see Table II). Observed x-ray emission from the fuel region further supports this conclusion.

The irradiation nonuniformity of $\simeq25\%$ in this experiment can cause a fuel-radius variation having an amplitude of the order of the mean fuel radius of $\simeq100$ μm. This radius was estimated from the observed fuel areal density. The amplitude may be large enough for the pusher to be mixed with the fuel. To estimate a shell thickness perturbation grown by Rayleigh-Taylor (RT) instability, we assume that the initial perturbation is amplified until the amplitude is equal to the shell thickness and then RT spikes fall freely in the frame of the accelerated shell. For the most sensitive wavelength (approximately equal to shell thickness), the initial surface roughness of $\simeq0.02$ μm in this experiment may be increased to an amplitude of the order of the fuel radius. (We used the RT growth rate reduced from a classical

value by a factor of $\simeq 2$.[12,13]) This amplitude then sets an initial perturbation of further instability in the shell deceleration phase. It appears, therefore, that the enhanced energy loss is due to fuel-pusher mixing originating from irradiation nonuniformity and/or RT instability.

It would be worthwhile to estimate a degree of the fuel-pusher mixing. Such mixing may be characterized by a fuel purity, $X \equiv \rho_D/\rho_{tot}$, given by the ratio of deuteron density to total fuel density, including pusher mass mixed in the fuel. In addition to the previous assumption of the uniform temperature and density profiles, it is assumed that the fuel purity is also spatially uniform. Since the energy loss is due mainly to Coulomb collisions with electrons, this loss is approximately proportional to $\rho_D R \ln\Lambda / X T_e^{3/2}$, where T_e is "real" electron temperature. Therefore, the method using secondary fusion reactions yields an experimental value for $X T_e^{3/2}/\ln\Lambda$. The unknown temperature T_e may be estimated by the further assumption that electrons with density n_D and the temperature T_{calc} (simulation result) are rapidly cooled by the cold pusher electrons having density Zn_p; then $T_e/T_{calc} = n_D/(n_D + Zn_p) = X$. Under these assumptions, the purity is estimated to be 0.25 ± 0.04 and $0.36^{+0.09}_{-0.08}$ for targets A and B, respectively.

In conclusion, charged-particle energy loss measured by the use of secondary fusion reactions was found to be strongly enhanced in comparison with results of hydrodynamic simulation. This enhancement arises from fuel-pusher mixing which reduces the fuel mass purity to roughly 30%.

The authors wish to express their gratitude to Dr. S. Morinobu for his valuable discussions on the CR-39 calibration experiments carried out at the Research Center for Nuclear Physics, Osaka University. We also thank the Gekko XII operation crew and the target fabrication group.

[1]N. M. Ceglio and L. W. Coleman, Phys. Rev. Lett. **39**, 20 (1977); J. S. Wark *et al.*, Bull. Am. Phys. Soc. **31**, 1417 (1986).

[2]E. G. Gamalii, S. Yu. Gus'kov, O. N. Krokhin, and V. B. Rozanov, Pis'ma Zh. Eksp. Teor. Fiz. **21**, 156 (1975) [JETP Lett. **21**, 70 (1975)]; T. E. Blue *et al.*, J. Appl. Phys. **54**, 615 (1983).

[3]H. Azechi *et al.*, Appl. Phys. Lett. **49**, 555 (1986).

[4]N. Miyanaga *et al.*, Rev. Sci. Instrum. **57**, 1731 (1986).

[5]R. O. Stapf *et al.*, Institute of Laser Engineering Research Report No. ILE 8704P, 1987 (to be published).

[6]M. D. Cable *et al.*, Bull. Am. Phys. Soc. **31**, 1461 (1986).

[7]K. Nishihara, R. Tsuji, and H. Azechi, Jpn. J. Appl. Phys. Pt. 2 **26**, L1301 (1987); H. Azechi *et al.*, Bull. Am. Phys. Soc. **31**, 1417 (1986).

[8]M. D. Cable and S. P. Hatchett, J. Appl. Phys. **62**, 2233 (1987).

[9]D. W. Shivukhin, *Review of Plasma Physics* (Consultants Bureau, New York, 1966), Vol. 4, p. 93.

[10]R. O. Stapf *et al.*, Nucl. Instrum. Methods Phys. Res., Sect. A **254**, 135 (1987).

[11]T. Yabe *et al.*, Nucl. Fusion **21**, 803 (1981).

[12]A. J. Cole *et al.*, Nature (London) **299**, 329 (1982); J. Grun *et al.*, Phys. Rev. Lett. **53**, 1352 (1984); J. S. Work *et al.*, Appl. Phys. Lett. **48**, 969 (1986).

[13]B. J. Daly, Phys. Fluids **10**, 297 (1967); H. Takabe, K. Mima, L. Montierth, and R. L. Morse, Phys. Fluids **28**, 3676 (1985), and references therein.